JACC Vol. 5, No. 3
March 1985:625–31

Spatial Variation of QT Intervals in Normal Persons and Patients With Acute Myocardial Infarction

DAVID M. MIRVIS, MD

Memphis, Tennessee

The QT interval is a clinically important electrocardiographic measurement. This study attempted to determine 1) whether this interval was spatially distributed in a physiologically meaningful way on the torso of normal subjects, and 2) if these spatial patterns were altered in patients with acute myocardial infarction. To do so, 30 patients were studied within 72 hours of the onset of acute myocardial infarction (15 with an anterior and 15 with a posterior lesion) along with 50 normal control subjects. Electrocardiographic signals were registered from 150 torso electrodes; the QT interval in each lead was determined by a combined automated-manual method, and the durations displayed as "isointerval maps."

In the normal subjects, the difference between the longest and shortest interval in each case was 59.4 ± 12.9 ms. Long QT intervals were spatially located over the left lateral torso and short QT intervals were found over the right inferior chest. Acute infarction modified this distribution in relation to lesion location; the longest QT intervals were centrally positioned in anterior infarction and caudally located in inferior infarction. Thus, QT intervals in normal and abnormal states have distinctive spatial distributions that are consistent with known regional myocardial electrophysiology.

(J Am Coll Cardiol 1985;5:625–31)

The QT interval is a clinically important electrocardiographic measurement. Prolonged intervals have been found in congenital (1), acquired (1,2) and drug-induced (3) conditions which predispose to development of complex and often fatal cardiac arrhythmias. This relation may be based on the dependence of both the QT interval (4) and arrhythmogenesis (5,6) on increased disparities in ventricular recovery times.

The duration of electrical systole, the simplest correlate of the QT interval, varies from one cardiac region to another (7–10), and many of the cardiac anatomic and functional states associated with a prolonged QT interval are regional in nature. Other electrophysiologic variables that are also regionally distributed have body surface electrocardiographic projections that are similarly distributed. For example, surface patterns have been shown to correlate with locations of infarction (11,12) and sites of anomalous bypass tracts (13).

From the Division of Cardiovascular Diseases, University of Tennessee Center for the Health Sciences and Veterans Administration Medical Center, Memphis, Tennessee. This project was supported by Grants HL00560 and HL20597 from the National Heart, Lung, and Blood Institute, National Institutes of Health, Bethesda, Maryland. Manuscript received May 14, 1984; revised manuscript received July 11, 1984, accepted September 6, 1984.

Address for reprints: David M. Mirvis, MD, 956 Court Avenue, Room 2F18, Memphis, Tennessee 38163.

Because of this successful and meaningful experience with other regional electrophysiologic effects such as myocardial ischemia (11,12), we examined the spatial distribution of the QT interval. A healthy group of subjects was evaluated to define the normal spectrum of distribution and another group with acute myocardial infarction was studied to examine the effects of regional pathophysiology on these patterns.

Methods

Study groups. Two sets of subjects were studied. First, a group of 50 normal men, aged 18 to 34 years, was evaluated. None had cardiovascular symptoms, and each had normal physical examination, electrocardiogram and chest X-ray film. All were normotensive and none was taking any cardioactive medications or diuretic drugs.

A second group of 30 patients, aged 38 to 74 years, was studied 24 to 72 hours after having an acute myocardial infarction. Infarction was diagnosed by standard criteria (14), with typical QRS and ST-T abnormalities but without bundle branch block. Fifteen of the 30 patients had acute inferior and the other 15 had acute anterior lesions as determined by usual electrocardiographic variables. At the time of study, none of these patients was being treated with digitalis glycosides or antiarrhythmic agents; serum elec-

0735-1097/85/$3.30

JACC Vol. 5, No. 3
March 1985:625–31

trolytes (potassium, calcium and magnesium) and arterial pH and partial pressure of oxygen (Po_2) were within clinically acceptable limits in all patients. Voluntary, informed written consent was obtained before the study.

Electrode system. Electrocardiographic signals were registered from 150 chloridized silver electrodes positioned on the anterior and posterior torso from the level of the clavicles to below the inferior rib margin (14,15). One hundred electrodes were located anterior and 50 were located posterior to the posterior axillary lines. Additional electrodes were placed on the limbs to record bipolar and unipolar limb leads and to derive a Wilson central terminal voltage.

Data acquisition. Signals were amplified by a bank of 33 low noise, differential (grid potential versus Wilson central terminal voltage) amplifiers. Gains (1,000 to 16,000×) and offsets were individually set under computer control (16) so that output filled the input range of the analog to digital converter.

Electrocardiographic signals were acquired in five sets. Each set consisted of 30 torso electrode potentials plus standard leads I, II and III. These three standard leads, recorded with each of the five data sets, verified the stability of the recordings during acquisition and documented the correct merging of the data sets (14,15).

A 20 second sample of each of the five electrode groups was digitized at a sampling rate of 500 samples/channel per second. Baseline stability was carefully determined during data acquisition by oscilloscopic observation of records.

Data processing. The five data sets were merged and individual grid electrode waveforms were averaged to yield one set of 150 unipolar thoracic electrocardiograms. Data sets were time-aligned using a hard-wired QRS trigger whose output was recorded along with the electrocardiographic data (14,15). Beats to be averaged were chosen by an automated numerical routine comparing one PQRST waveform with another, generating a value or "waveform index" of unity if the two were identical; cycles with indexes of 0.8 to 1.2 were selected for averaging (14,15).

QRS onset and T wave offset were determined separately for each of the 150 torso and 12 standard leads. First, onset and offset of the QRS and ST-T waves were manually selected from root-mean-square potential plots. These points were used to identify a terminal TP segment baseline and as initial estimates in the next stage. This second stage included automated detection of QRS onset and T wave offset for each lead. The onset of the QRS complex was defined as the instant at which the potential slope exceeded twice that of the preceding 10 ms of the PR segment. The end of the T wave was defined as the instant at which potentials during 6 ms deviated from those predicted by a linear fit of 10 ms of the immediately following TP segment. Third, data for each lead were visually examined and edited manually; approximately 15% of the leads required editing. The onset of the QRS complex and offset of the T wave were timed in relation to the output of the hard-wired QRS trigger recorded with each data set. The QT interval was computed as the difference between these two points, expressed as milliseconds.

Two methods were used to compare QT intervals from different torso sites. For comparison of one locus with another in the same subject, actual intervals were plotted as "isointerval maps," with contour lines connecting points with equal durations. Because QT intervals varied widely from subject to subject, a second statistically based method was used in which the QT interval at each site was converted to a standard deviate (or Z score) as defined by:

$$Z = (Ii - \mu)/\sigma),$$

where Ii = QT interval at site i, μ = mean of all 150 Ii values and σ = standard deviation of the 150 interval values (17). When plotted as "isodeviate maps" using contour lines to connect sites with QT intervals that were an equal number of deviations from the mean value of all 150 QT intervals of that map, areas with short and long intervals could be identified.

Statistics. All data were expressed as mean ± 1 standard deviation. Differences between groups were evaluated using two-way analysis of variance (17), with a 1% significance level.

Results

Normal Subjects

Range of QT interval duration. In the 50 normal subjects, QT intervals varied from person to person. Values for all 150 intervals in each subject varied from 335.5 to 486.6 ms (mean 384.1 ± 39.7). The longest QT interval in any one lead varied from 371 to 514 ms (mean 414.4 ± 29.6).

QT interval and torso site. Similarly, QT interval measurements from the 150 torso sites varied widely within any one subject. The difference between the shortest and longest intervals in individual cases varied from a minimum of 34 ms to a maximum of 88 ms (mean 59.4 ± 12.9). Variances about the mean varied from 42.3 to 313.9 ms^2 (mean 163.6 ± 69.5). Thus, there was a significant range of QT intervals when measured from different torso sites in any one subject.

Examples of two QRST waveforms illustrating these results are shown in Figure 1. The QT interval registered from a left precordial electrode in a normal subject measured 384 ms. That of the waveform recorded from a right torso site of the same subject measured only 336 ms.

Spatial measurement of QT interval. We next sought to determine if these ranges of intervals were spatially distributed in a consistent manner. To do so, we first constructed "isointerval maps," as described earlier. An example from one normal subject is presented in Figure 2.

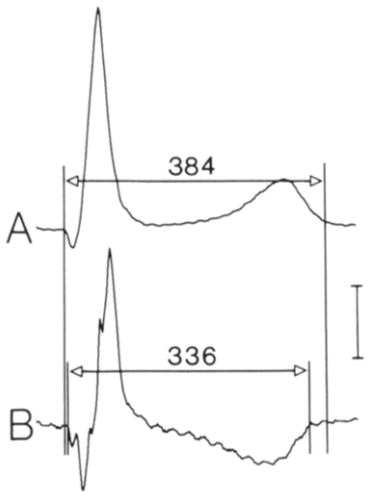

Figure 1. Two QRST waveforms from one normal subject illustrating regional differences in QT intervals. **Vertical lines** mark selected QRS onsets and T wave offsets in each lead, defining the QT interval. Durations of this interval in each record are tabulated (in ms). The scale figure (**right margin**) corresponds to 500 μV for waveform A (recorded from the left lateral precordium) and 100 μV for waveform B (recorded from the right lateral chest).

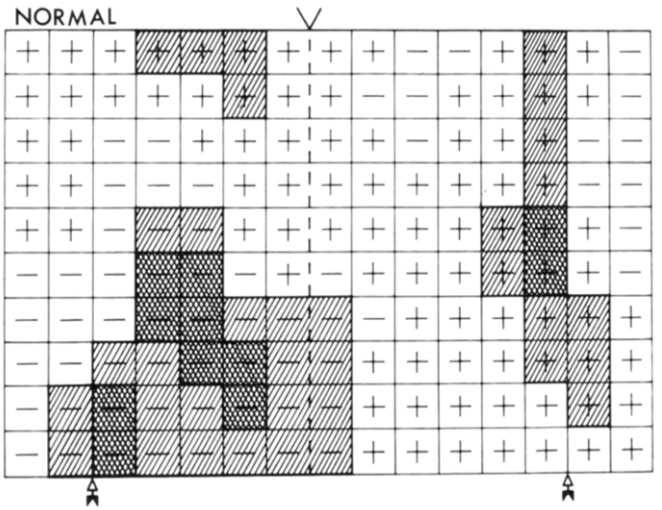

Figure 3. "Isodeviate map" computed from data of normal subjects of Figure 2, as described in the text. **Plus and minus signs** mark electrode locations with QT intervals greater than or less than the mean of all 150 electrode values. Regions with a standard deviate of greater than ± 1.0 are **lightly shaded**; those with magnitudes greater than ± 2.0 are **heavily shaded**. Map orientations are as in Figure 2.

The QT intervals at all sites in this case measured 336.4 ± 13.9 ms (range 324 to 384). The longest intervals were recorded from the left lateral and posterior torso and a smaller zone on the right superior chest wall, whereas the shortest intervals were measured from sites over the right inferior chest wall.

To facilitate comparisons among cases, intervals were converted to standard deviates (17). An "isodeviate map," constructed from data presented earlier is shown in Figure 3. Measurements were less than the mean value of 366.4 ms on the right inferior chest wall and on a small zone on the left upper torso; intervals were greater than the mean over the remainder of the chest. Within each of these areas, smaller regions with more extreme measures, that is, with standard deviations of greater than 1 and 2 were identified.

Data from the entire group of 50 subjects demonstrated similar results. Z scores of each torso site were averaged for all cases. Values ranged from −1.56 to 1.05. The spatial distribution of these mean values is depicted in Figure 4. Lowest scores, corresponding to the shortest QT intervals,

370	372	378	380	380	380	376	374	370	364	366	376	380	370	364
376	374	372	370	372	380	376	378	362	364	370	378	380	368	360
374	372	366	362	372	376	376	378	368	366	378	378	380	366	362
368	372	366	364	358	372	378	376	370	378	374	376	380	364	362
368	368	366	340	346	368	370	370	370	378	374	380	382	372	360
360	366	364	332	330	366	368	366	370	374	378	380	384	376	360
362	364	360	332	324	346	344	356	366	368	376	378	380	380	370
362	354	352	348	328	332	348	358	372	368	376	378	380	380	370
362	346	336	358	352	332	352	354	370	374	376	378	378	380	372
364	346	336	346	352	350	352	360	370	378	374	376	376	378	374

Figure 2. "Isointerval map" depicting the QT intervals (in ms) at each of 150 locations in one normal subject. The center of the map (**dashed line,** ⋁) is along the sternum, with the right and left borders corresponding to the left and right paravertebral zones, respectively. **Arrows** mark the two posterior axillary lines. Zones with the longest (≥ 380 ms) QT intervals are **diagonally striped**; those with the shortest (< 340 ms) QT intervals are **horizontally striped**.

JACC Vol. 5, No. 3
March 1985:625–31

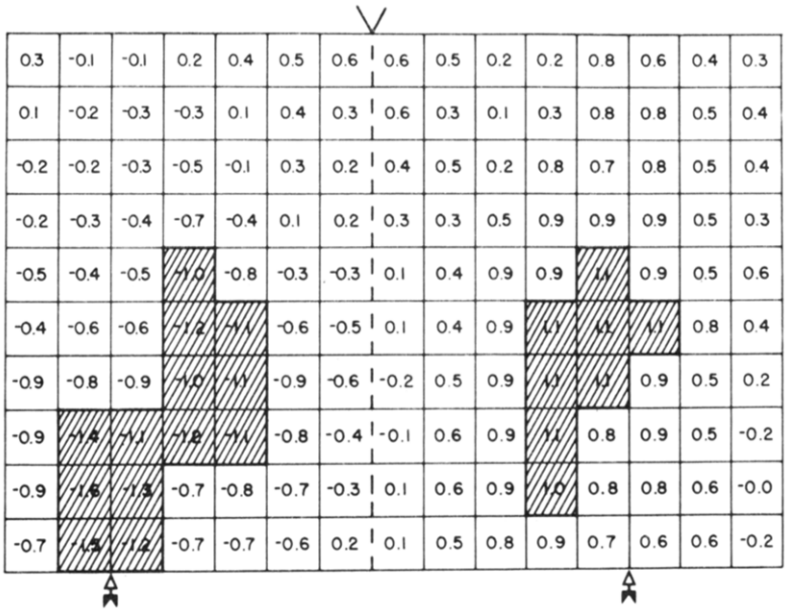

Figure 4. Spatial distribution of mean values of standard deviates at the 150 torso location in the 50 normal subjects. Regions with mean values of greater than ± 1.0 are **shaded**. The map is oriented as in the previous figures.

were located over the right inferior chest wall. Highest scores, corresponding to the longest QT intervals, were observed over the left lateral torso.

Determinants of QT duration. In normal subjects, QT intervals recorded from 150 torso sites varied widely, but in a consistent spatial distribution with the longest intervals on the left and shortest intervals on the right hemithoraces. This spatial variation may have two components, namely, differences in onset of the QRS complex and differences in end of the T wave. To determine which was the major factor resulting in QT interval variations, the variances (17) of the timing of the two instants (referenced to the QRS trigger output) about the mean value for the 150 leads of each case was computed. Variances in onset of the Q wave ranged from 9.3 to 43.4 ms^2 in the 50 cases; that of the end of the T wave varied from 39.9 to 254.4 ms^2. In each case, the variance of timing of the end of the T wave in the 150 leads was significantly greater (F test, $p < 0.001$) than that of the onset of the QRS complex. An example of the greater variability in ending of the T wave than beginning of the QRS complex is seen in Figure 1. The ratio of the variance of QT interval duration in the 150 leads of each case to that of the QRS onset was likewise significantly greater (F test, $p < 0.01$) than unity in each case; however, that of QT interval variance to T wave offset variance was not significantly different from unity ($p > 0.1$). Thus, variation in T wave termination, rather than in QRS complex beginning, is the major determinant of the QT interval range.

Acute Myocardial Infarction

Anterior infarction. Fifteen patients were studied within 72 hours of acute anterior myocardial infarction. Mean values of QT intervals in the 150 torso leads were 416.7 ± 46.1 ms (range 376.4 ± 476.4); this value was not significantly different ($p > 0.1$) from the normal values. The longest interval (476.3 ± 32.1 ms) was, however, significantly longer than normal.

A representative example of a QT "isodeviate map" derived from one subject in this group is shown in Figure 5A. As in normal persons, QT intervals showed a wide spatial variation, with individual values ranging from 318 to 459 ms (mean 396.7 ± 28.9). However, in contrast to normal subjects, the zone with the longest QT intervals was located centrally rather than laterally. This pattern was observed in all patients with acute anterior infarction.

Inferior infarction. A different pattern was seen in the 15 subjects studied within 72 hours of an acute inferior infarction. Values of the 150 torso QT intervals ranged from 369.4 to 467.3 ms (mean 408.7 ± 34.2). Maximal intervals measured 464.6 ± 27.4 ms and were significantly larger than normal, but not different from those of subjects with anterior infarction.

A QT "isodeviate map" from one member of this group is shown in Figure 5B. The longest QT intervals were located inferiorly on the anterior torso along a horizontal axis.

Spatial distribution. Intervals for each case in these two groups were converted to standard deviates and averaged, as done in the normal subject group (Fig. 4). Zones with mean values of 1 or greater for the normal set and for the two subsets with acute infarction are overlayed in Figure 6. The areas of the longest QT intervals differ among the three groups, with that of anterior infarction being central to and that of inferior infarction lying caudal to that of the normal control subjects.

Variations in QRS onset in the 150 leads of each subject were significantly less ($p < 0.001$) than that of T wave

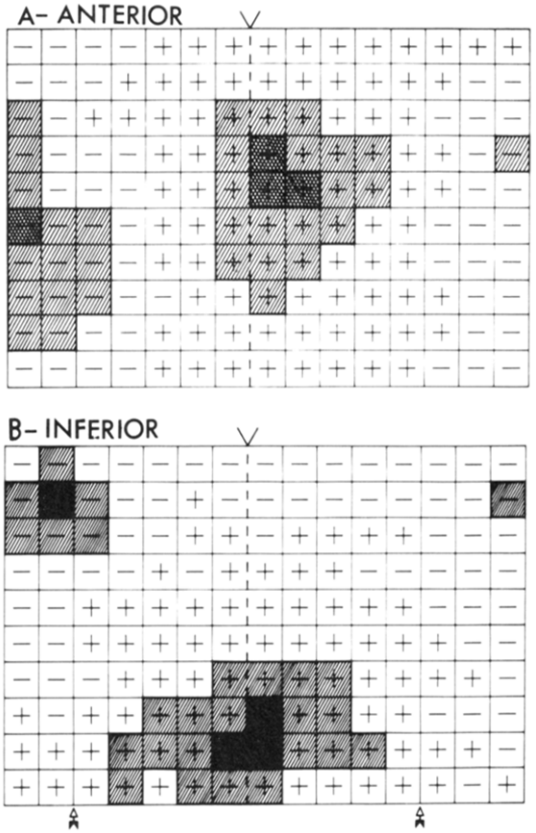

Figure 5. Isodeviate maps, constructed as in Figure 3, from two patients, one with an acute anterior (**A**) and one with an acute inferior (**B**) myocardial infarction. The **lightly shaded areas** had standard deviates of ± 1 or greater; **heavily shaded areas** had standard deviates of ± 2 or greater.

offset. Neither variance was different from that in normal subjects.

Discussion

This study demonstrates that QT intervals are spatially distributed on the torso in a reproducible manner, and that these patterns are altered by regional myocardial disorders. These findings will be examined in relation to methodologic concerns, electrophysiologic mechanisms and clinical implications.

Methodology. Accurate determination of the QT interval, particularly the end of the T wave, is very complex. Problems, as discussed by Lepeschkin and Surawicz (18), include: 1) exact demarcation of the beginning of the QRS complex and end of the T wave, and 2) incorrect separation of T and U waves. Total exclusion of the latter is difficult, particularly using automated algorithms that may assume certain forms for the end of the T wave (19,20). We attempted to control this by combined application of computer processing to expedite the study of 150 leads per subject and manual editing to reduce errors. Measured QT intervals were not adjusted for rate; we were primarily interested in differences in interval duration in each subject, rather than differences among subjects.

The former problem has three subcomponents. First, precise identification of the beginning or ending of any waveform is dependent on the gain used to study the complex. Second, the accuracy of interval measurements is dependent on a stable electrical baseline. These were approached in this effort by individual gain settings for each lead filling the input range of the analog to digital converter, and by selective beat averaging and linear baseline drift correction after visual verification of stability during data acquisition. Both would be of greater significance in QRST area computations (21), in which timing errors are multiplied by voltage amplitudes.

The third subcomponent, namely, inclusion of isoelectric initial or terminal segments (or both) of the QRST interval, is particularly important. If one views global, instantaneous cardiac activity as being generated by a single dipole, then zero potential will be recorded at loci perpendicular to the dipole axis. This interpretation has two deficiencies. First, cardiac activity, particularly during the QRS complex, cannot be adequately represented by a single dipole (22). Second, lumping all activity into one or more global equivalent cardiac generators ignores the regional or "proximity" electrocardiographic effects that have been repeatedly demonstrated (11,23).

Remote versus local potentials. A second interpretation is based on these regional projections. No electrical activity will be recorded from surface sites to which a spe-

Figure 6. Overlay of surface areas with averaged standard deviates of unity or greater for normal subjects (labeled N) and for those with acute anterior (A) and inferior (I) myocardial infarction. **Asterisks** mark electrode sites at which deviations were less than unity for all three groups of patients.

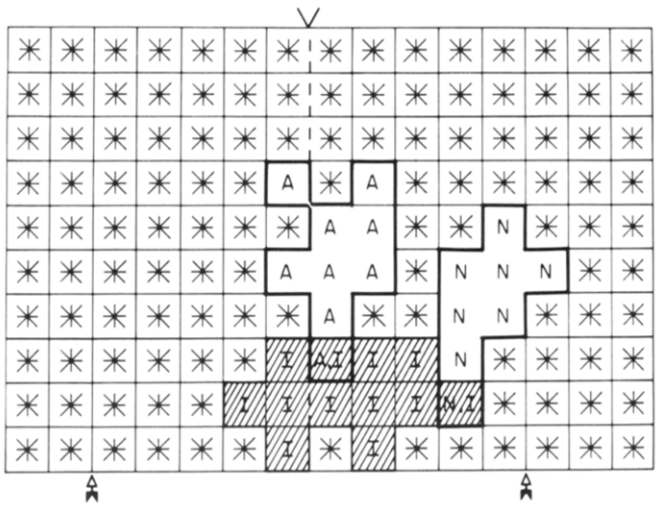

JACC Vol. 5, No. 3
March 1985:625–31

cific region or regions project activity when these zones are inactive. This may be before activation begins or after recovery is completed in certain but not all cardiac elements. Thus, regional but not global activity is absent, and it is the proximity of a lead to specific regions, rather than its orientation to a mean cardiac dipole, that results in isoelectricity.

Two constraints do, however, exist. First, distant activity does influence local potentials. The magnitude of this contamination will vary in proportion to the magnitudes of the local and remote forces and their relative distances from the recording site. Thus, initial Q waves defining the onset of the QT interval in certain leads reflect remote rather than local activation. Second, the "intrinsicoid deflection" (24,25), that is, the peak negative dV/dt during the QRS complex, rather than the onset of the QRS complex, corresponds with local cardiac excitation. Thus, the QT interval recorded from a certain body surface or epicardial lead does not totally reflect the duration of regional electrical systole.

Normal variations in QT intervals. *Onset of QRS.* Acknowledging these limitations, our results in normal subjects may be interpreted in accordance with prior electrophysiologic studies. The sequence of ventricular excitation in canine and human hearts has been repeatedly described (7). Although correlations between epicardial QRS wavefronts and body surface waveforms do exist, the resulting temporal variations are of secondary importance in generating the surface QT interval spatial patterns. This was suggested by the significantly smaller variance in QRS complex onset than in T wave offset or in QT interval duration. One explanation is the inclusion of distant as well as local cardiac forces in the surface lead QRS complex, as exemplified by initial negativity (Q waves) that reflects oppositely directed, relatively strong activation forces in opposite cardiac structures. Thus, the onset of the QT interval is dependent on global effects and is thereby less sensitive to regional events.

Regional differences in refractory and recovery times. Studies using refractory periods (8,9,26) and monophasic action potentials (10) to define action potential durations have also identified a sequence of ventricular recovery. Burgess et al. (8) and Abildskov (9) reported that functional refractory periods are longer at the apex than at the base of the left ventricle; values recorded over the right ventricular epicardium were shorter or equal to those recorded over the left ventricle. Isochrone maps of recovery "wavefronts" constructed from monophasic action potentials by Toyoshima et al. (10) demonstrated that repolarization was first completed in the midportion of the right ventricular free wall; the apex and a portion of the basal left ventricle were the last to complete recovery.

These regional differences in recovery times are the likely cause of the described spatial QT intervals. This is supported by the greater variance in T wave offsets than QRS onsets and by the insignificant differences between variances of QT intervals and T wave endings.

The observed QT interval patterns do correspond with the recovery sequences as outlined. Short intervals recorded over the right side of the chest relate to short refractory periods and monophasic action potentials recorded over the right ventricle. Long QT intervals recorded over the left lateral torso correspond to long values recorded over the lateral and apical left ventricle.

Effects of acute infarction. Prior studies (27,28) documented changes in the QT interval after acute myocardial infarction. After a brief initial shortening (28), the QT interval prolongs (27,28). This abnormality is particularly common in patients who have a sudden cardiac death (2).

Mechanisms. Although the mechanisms for these effects are not clear, they do relate to experimental electrophysiologic data. Action potential durations, directly recorded or estimated from refractory period measurements, shorten promptly after coronary ligation (29–31). After 1 day, however, action potential durations and refractory periods are abnormally prolonged (29,32). Such prolongation has been reported in human infarcted myocardium excised at the time of transplantation (33). Thus, the biphasic response of the QT interval, correlating with the biphasic effects of ischemia on action potential durations (26), would be anticipated. It is probable that patients in our study were evaluated during the later phase of this evolution.

Data presented here extend the findings of prior experimental and clinical reports. Even though the mean value of the QT interval was not prolonged in patients after infarction, the spatial distribution of the QT intervals was clearly abnormal. The shift in sites of the longest intervals (Fig. 4 and 5) to regions roughly approximating the surface projection of the cardiac damage is consistent with the experimentally defined regional prolongation of action potential durations. The QT interval at these sites may be further prolonged by an increased activation time (34), further delaying the end of the action potential.

Clinical implications. These data further document the ability of body surface mapping techniques to detect regional myocardial abnormalities. In addition to the ability of these techniques to identify normal amplitude and spatial electrocardiographic patterns (35) and abnormalities occurring after acute infarction (14), the results illustrate their ability to depict normal and abnormal regional deviations in ventricular recovery times. Such data may be complementary to that gained by isoarea or isointegral mapping methods (6,36). Because excessive dispersion of recovery times increases the susceptibility to malignant arrhythmias (5,6), the more complete assessment of this variable afforded by this and analogous noninvasive methods may be useful in identifying clinical states at risk of sudden death.

References

1. Moss AJ, Schwartz PJ. Delayed repolarization (QT and Q-U prolongation) and malignant ventricular arrhythmias. Mod Concepts Cardiovasc Dis 1982;51:85–90.

2. Schwartz PJ, Wolf S. QT interval prolongation as predictor of sudden death in patients with myocardial infarction. Circulation 1978;57:1074–7.
3. Reynolds EW, Vander Ark CR. Quinidine syncope and delayed repolarization syndromes. Mod Concepts Cardiovasc Dis 1976;55:117–22.
4. Abildskov JA. Adrenergic effects on the QT interval of the electrocardiogram. Am Heart J 1976;92:210–6.
5. Han J, Moe GK. Nonuniform recovery of excitability in ventricular muscle. Circulation 1964;14:44–60.
6. Abildskov JA, Burgess MJ, Urie PM, Lux RL, Wyatt RF. The unidentified content of the electrocardiogram. Circ Res 1977;40:3–7.
7. Spach MS, Barr RC. Ventricular intramural and epicardial potential distributions during ventricular activation and repolarization in the dog. Circ Res 1975;37:243–57.
8. Burgess MJ, Green LS, Millar K, Wyatt R, Abildskov JA. The sequence of normal ventricular recovery. Am Heart J 1972;84:660–9.
9. Abildskov JA. The sequence of normal recovery of excitability in the dog heart. Circulation 1975;52:442–6.
10. Toyoshima H, Lux RL, Wyatt RF, Burgess MJ, Abildskov JA. Sequences of early and late phases of repolarization of dog ventricular epicardium. J Electrocardiol 1981;14:143–52.
11. McLaughlin VW, Flowers NC, Horan LG, Killam HAW. Surface potential contribution from discrete elements of ventricular wall. Am J Cardiol 1981;34:302–8.
12. Mirvis DM. Differential electrocardiographic effects of myocardial ischemia induced by atrial pacing in dogs with various locations of coronary stenosis. Circulation 1983;68:1116–26.
13. DeAmbroggi L, Taccardi B, Macchi E. Body surface maps of heart potentials: tentative localization of pre-excited areas in forty-two Wolff-Parkinson-White patients. Circulation 1976;54:251–63.
14. Mirvis DM. Body surface distributions of repolarization forces during acute myocardial infarction. I. Isopotential and isoarea mapping. Circulation 1980;62:878–87.
15. Mirvis DM. Body surface distribution of electrical potential during atrial depolarization and repolarization. Circulation 1980;62:167–73.
16. Cox JW, Laughter JS, Brandon CW, et al. A systems oriented ECG amplifier. Cardiovasc Res 1979;13:238–41.
17. Sokal RR, Rohlf FJ. Biometry. San Francisco: Freeman, 1969:99–106.
18. Lepeschkin E, Surawicz B. The measurement of the Q-T interval of the electrocardiogram. Circulation 1952;6:378–88.
19. O'Donnell J, Knoebel SB, Lovelace DE, McHenry PL. Computer quantitation of Q-T interval and terminal T wave (aT-eT) intervals during exercise: methodology and results in normal men. Am J Cardiol 1981;47:1168–72.
20. Puddu PE, Bernard PM, Chaitman BR, Bourassa MG. QT interval measurement by a computer assisted program: a potentially useful clinical parameter. J Electrocardiol 1982;15:15–22.
21. Wilson FN, Macleod AG, Barker PS, Johnston FD. The determination and the significance of the areas of the ventricular deflections of the electrocardiogram. Am Heart J 1934;10:46–61.
22. Mirvis DM, Keller FW, Cox JW. Experimental comparison of four inverse electrocardiographic constructs in the isolated rabbit heart. J Electrocardiol 1978;11:57–65.
23. Abildskov JA, Burgess MJ, Lux RL, Wyatt RF. Experimental evidence for regional influence in body surface isopotential maps in dogs. Circ Res 1976;38:386–91.
24. Wilson FN, Johnston FD, Cotrim N, Rosenbaum FF. Relations between the potential variations of the ventricular surfaces and the form of the ventricular electrocardiogram in leads from the precordium and the extremities. Trans Assn Am Phys 1941;56:258–71.
25. Spach MS, King TD, Barr RC, Boaz DE, Morrow MN, Herman-Giddens S. Electrical potential distribution surrounding the atria during depolarization and repolarization in the dog. Circ Res 1969;24:857–73.
26. Martins JB, Zipes DP, Lund DD. Distribution of local repolarization changes produced by efferent vagal stimulation in the canine ventricles. J Am Coll Cardiol 1983;2:1191–9.
27. Doroghazi RM, Childers R. Time-related changes in the Q-T interval in acute myocardial infarction: possible relation to local hypocalcemia. Am J Cardiol 1978;41:684–8.
28. Cinca J, Figueras J, Tenorio L, et al. Time course and rate dependence of Q-T interval changes during noncomplicated acute transmural myocardial infarction in human beings. Am J Cardiol 1981;48:1023–8.
29. Mandel WJ, Burgess MJ, Neville J, Abildskov JA. Analysis of T-wave abnormalities associated with myocardial infarction using a theoretic model. Circulation 1968;38:178–88.
30. Lazzara R, El-Sherif N, Scherlag BJ. Early and late effects of coronary artery occlusion on canine Purkinje fibers. Circ Res 1974;35:391–9.
31. Downar E, Janse MJ, Durrer D. The effect of acute coronary artery occlusion on subepicardial transmembrane potentials in the intact porcine heart. Circulation 1977;56:217–23.
32. Lazzara R, El-Sherif N, Scherlag BJ. Electrophysiologic properties of canine Purkinje cells in one-day-old myocardial infarction. Circ Res 1973;33:722–34.
33. Dangman KH, Danilo P, Hordof AJ, Mary-Rabine L, Reder RF, Rosen MR. Electrophysiologic characteristics of human ventricular and Purkinje fibers. Circulation 1982;65:362–8.
34. Boineau JP, Cox JL. Slow ventricular activation in acute myocardial infarction: a source of re-entrant premature ventricular contraction. Circulation 1973;48:702–13.
35. Spach MS, Barr RC, Warren RB, Benson DW, Walston A, Edwards SB. Isopotential body surface mapping in subjects of all ages: emphasis on low-level potentials with analysis of the method. Circulation 1979;59:805–21.
36. Montague TJ, Smith ER, Spencer CA, et al. Body surface electrocardiographic mapping in inferior myocardial infarction. Circulation 1983;67:665–73.